

Switching on and off two-photon absorption in nanoparticles doped in polaritonic materials

Mahi R. Singh

Department of Physics and Astronomy, The University of Western Ontario, London, Ontario N6A 3K7, Canada

(Received 20 December 2006; revised manuscript received 27 February 2007; published 23 April 2007)

A theory of nonlinear two-photon absorption has been developed for a polaritonic band-gap material doped with an ensemble of three-level nanoparticles. We have considered that the nanoparticles are interacting with the polaritonic material. An expression of two-photon absorption has been obtained by using the density-matrix method. The effect of the dipole-dipole interaction (DDI) has also been included in the formulation, which leads to interesting phenomena. For example, it has been found that the two-photon absorption can be turned on and off when the decay resonance energy of the three-level nanoparticles is moved within the lower-energy band. It has also been found that the inhibition effect can also be achieved by controlling the strength of the DDI.

DOI: [10.1103/PhysRevB.75.155427](https://doi.org/10.1103/PhysRevB.75.155427)

PACS number(s): 73.21.-b, 78.67.Hc, 71.35.Gg, 42.50.Ct

I. INTRODUCTION

There is a considerable interest in the study of the electronic and photonic properties of nanoparticles doped in different materials.¹⁻¹² For example, nanoparticles such as quantum dots are doped in semiconductors,²⁻⁴ dielectric media,⁵ macrocavities,⁶ liquids,⁷ dispersing and absorbing materials,⁸ low-temperature solids,⁹ oxide materials,¹⁰ organic materials,¹¹ and photonic crystals.¹²

One of the most intriguing possible applications of nanoparticles is that they may be used to build quantum computers.¹ Nanoparticles are quantum heterostructures which are composed of nanoscale regions of one type of material embedded in a material of another type. The electrons are confined within the nanoparticle region. Therefore, the confined electronic energy levels can be accurately controlled by varying the particle's size, shape, or composition and the number of confined electrons. Nanoparticles such as quantum dots are also called artificial atoms or superatoms and have atomlike properties.^{2,3}

The aim of the present work is to study two-photon absorption in nanoparticles doped in polaritonic band-gap materials. The effect of the dipole-dipole interaction (DDI) has also been included in the calculations. Examples of polaritonic materials include semiconductors (i.e., Ge, GaAs, SiC), oxide crystals (i.e., MgO), ionic solids (i.e., NaF), etc.^{13,14} These materials have energy gaps in their polaritonic energy spectra due to the coupling between photons and optical phonons. The presence of energy gaps has led to the prediction of many interesting phenomena such as polariton-atom bound states,¹⁴ superradiance,¹⁵ electromagnetically induced transparency (EIT),¹⁶ etc.

DDI has been investigated in nanoparticles when they are doped in different host materials.^{5-9,17-23} For example, Wuisster *et al.*⁵ have measured the effect of the DDI on the spontaneous emission rate in CdTe and CdSe quantum dots doped in dielectric media. They found that it enhances the spontaneous emission rate and suggested that quantum dots can be used for testing DDI theories. On the other hand, Wang and Shih⁶ have performed time-resolved photoluminescence measurements to study DDI in quantum dots doped in planar cavity. They observed an increase of the energy transfer rate

in the microcavity compared to that measured in free space. This behavior was attributed to the DDI between the quantum dots.

Xu *et al.*⁷ have used photoluminescence to study the resonance energy transfer in CdTe quantum dots doped in a single water droplet. They found that DDI between dots is enhanced in the aqueous solution due to Brownian motion. However, Dung *et al.*⁸ have investigated the resonant DDI between two-level quantum dots doped in a dispersing and absorbing material. The dressed states created due to the DDI are responsible for forming qubits in the quantum processor. On the other hand, Petrosyan and Kurizki⁹ have proposed a high-performance quantum processor from pairs of two-level quantum dots doped in a low-temperature solid. They showed that the DDI between dots creates symmetric and antisymmetric states (i.e., dressed states).

DDI has also been investigated when quantum dots are doped in semiconductors. For example, Gea-Banacloche *et al.*¹⁷ have studied the effect of DDI in arrays of quantum dots. They showed that the dots act as three-level and four-level atoms in the presence of the DDI, and the EIT mechanism can be used for optical switching. On the other hand, Lovett *et al.*¹⁸ have developed an optical scheme for quantum computation in two-level quantum dots due to DDI. They showed that the switching can occur on a time scale which is much less than the typical decoherence times. Unold *et al.*¹⁹ have studied the DDI between two quantum dots and found an energy shift in the exciton spectrum and the Rabi oscillations. Sanders *et al.*²⁰ have proposed a quantum computer structure using strongly coupled quantum dots by utilizing the DDI effect.

DDI in local-field approximation has also been studied in nanoparticles.²¹⁻²³ For example, Empedocles and Bawendi²¹ have observed a large Stark shift in the lowest excited state due to the local field in CdSe quantum dots. They proposed that these dots can be used for electro-optic modulation devices. The effect of the local field on Rabi oscillations has also been studied in a quantum dot by Paspalakis *et al.*²² They have predicted possible population inversion in the system. The influence of electron-hole DDI in the local-field approximation has also been investigated by Slepian *et al.*²³ in a single quantum dot.

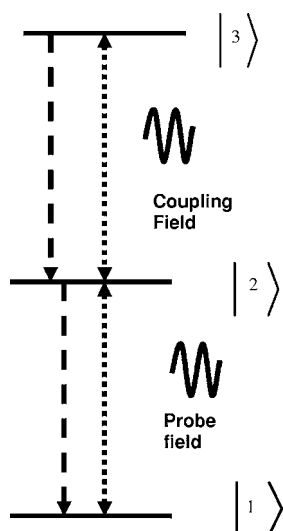


FIG. 1. A schematic diagram of a three-level nanoparticle. The levels are denoted by $|1\rangle$, $|2\rangle$, and $|3\rangle$. A probe laser couples levels $|1\rangle$ and $|2\rangle$ and a control laser couples levels $|2\rangle$ and $|3\rangle$. Levels $|3\rangle$ and $|2\rangle$ decay to levels $|2\rangle$ and $|1\rangle$, respectively.

DDI has also been studied extensively in quantum optics.^{24–28} It is found that when the density of multilevel atomic gases is high, the near DDI (i.e., the local-field effect) becomes important. The inclusion of the DDI between multilevel atoms has led to many interesting effects such as ultrafast optical switching,²⁵ intrinsic optical bistability,²⁶ enhancement of inversionless gain and absorptionless index of refraction,²⁷ and linear and nonlinear spectral shifts.²⁸

In the present work, we consider that an ensemble of nanoparticles is doped in a polaritonic crystal. The nanoparticles are interacting with the polaritonic material. The formulation of the two-photon absorption spectrum considers three-level nanoparticles. A coupling field is applied between the two excited states to control the two-photon process in the particles. A probe-laser field is applied between the ground state and the next excited state to measure the two-photon absorption spectrum. This type of experimental arrangement dealing with only three levels is called the cascade configuration in quantum optics.²⁹ In Fig. 1, a schematic diagram of a three-level particle is shown.

We consider that a dipole moment is created in each nanoparticle due to the transition between the two excited levels. This can be called the dipole moment due to the selected transition. The nanoparticles are densely doped in polaritonic crystals so that the particles are interacting with each other via the dipole-dipole interaction due to the selected transition (DDIST).

Recently, DDIST has also been studied in quantum optics^{30,31} and photonic crystals.³² For example, Lukin and Hemmer³⁰ have investigated the role of DDIST in three-level and four-level atoms. Their system consists of two atoms which are interacting with each other via the DDIST. The induced dipole in each atom is created due to one of the transitions in the atom. They predicted quantum entanglement between two atoms due to the DDIST. They suggested that the mechanism of this interaction can be used to produce quantum logic gates. The effect of the DDIST on quantum

jumps has also been investigated by Skornia *et al.*³¹ in two three-level atoms. In a previous paper, we have also studied the DDIST in photonic crystals doped with four-level atoms in the presence of three laser fields.³²

Expressions for the two-photon absorption spectrum (TPAS) have been obtained by using the density-matrix method in the presence and absence of DDIST. The effect of this interaction has been calculated using the mean-field approximation.^{33–35} Two-photon absorption has also been investigated for multilevel atoms in quantum optics.^{36,37} However, the effect of the DDI on the inhibition of two-photon absorption has not been investigated.

Numerical simulations have been performed for the SiC crystal which has a gap to midgap ratio of about 18%. The three levels of a nanoparticle are denoted by $|1\rangle$, $|2\rangle$, and $|3\rangle$, as shown in Fig. 1. These levels are taken in cascade configuration where two-photon absorption takes place. Levels $|2\rangle$ and $|1\rangle$ are driven by a probe-laser field, whereas a control laser field is applied between levels $|3\rangle$ and $|2\rangle$. It is considered that the nanoparticles are interacting not only with each other but also with the polaritonic material which is acting as a reservoir. Level $|3\rangle$ decays to level $|2\rangle$ due to the reservoir-nanoparticle coupling.

The following interesting phenomena are predicted by the present theory. It is found that as the DDIST coupling increases, the peak located at zero detuning splits into two peaks. These peaks are located on the right- and left-hand sides of the zero detuning point. The right-hand peak is stronger than the left peak. The heights of the peaks decrease as the DDI parameter increases. This means that the strength of the two-photon absorption process becomes weaker when the nanoparticles are interacting with each other via DDIST. At zero detuning, the spectrum of the two-photon absorption has a minimum which corresponds to the inhibition of two-photon absorption due to the DDIST. This is an interesting finding of the present work.

The mechanism behind two-photon inhibition due to DDIST can be explained by using a theory of dressed states. In the absence of DDIST, there are no dressed states in the system and only one route ($|1\rangle \rightarrow |2\rangle \rightarrow |3\rangle$) is available for the absorption of two photons. However, in the presence of DDIST, the system has two dressed states denoted by $|+\rangle$ and $|-\rangle$. Now, the system has two routes, $|1\rangle \rightarrow |-\rangle \rightarrow |3\rangle$ and $|1\rangle \rightarrow |+\rangle \rightarrow |3\rangle$, which are available for the two-photon absorption process. At zero detuning, the energy difference between two routes is zero. Therefore, these routes interfere with each other and the inhibition of two-photon absorption occurs.

We have also investigated the effect of the decay transition $|3\rangle \rightarrow |2\rangle$ on the TPAS. We see a very interesting result when the resonance energy gets near the band edge. It is found that the two absorption peaks in the spectrum merge into a single peak which is located at zero detuning. In other words, the inhibition of two-photon absorption disappears and the phenomenon of two-photon absorption can be switched on and off by tuning the resonance energy.

The phenomenon obtained in the present work can be used to advance toward the goal of producing logical photon switches for quantum information processing. These materials have unique advantages over conventional studies of EIT

in atomic gases and high- Q cavities.²⁹ The present study has at least two following main advantages. First, no control lasers are needed to create the quantum interference responsible for the energy splitting as in the EIT effect.²⁹ Second, the system parameters can easily be adjusted to provide a switching mechanism to turn the two-photon absorption on and off.

II. TWO-PHOTON ABSORPTION SPECTRUM (TPAS)

We consider that an ensemble of three-level nanoparticles is densely doped in a polaritonic material where the DDI between particles becomes important. Recently, nanoparticles such as quantum dots are used as multilevel atoms.^{2,3} The resonance energy in nanoparticles can be modified by varying the particles' sizes, shapes, or compositions, the number of confined electrons, external magnetic and/or electric fields,^{2,3} etc.

The particles are interacting with one another by the selected induced dipole transition $|2\rangle \leftrightarrow |3\rangle$. The DDI Hamiltonian for the nanoparticles is written as³³

$$H_d = \frac{1}{2} \sum_{i,j} \sum_{\alpha,\beta} J_{\alpha\beta}(\mathbf{r}_i - \mathbf{r}_j) \mu_\alpha(\mathbf{r}_i) \mu_\beta(\mathbf{r}_j), \quad (1)$$

$$J_{\alpha\beta}(\mathbf{r}) = \frac{\hat{r}_\alpha \hat{r}_\beta - \delta_{\alpha\beta}}{\epsilon_0 |\mathbf{r}|^3}, \quad (2)$$

where $\mu_\alpha(\mathbf{r}_i)$ is the α th component of the dipole moment of the i th nanoparticle. The function $J_{\alpha\beta}(\mathbf{r}_i - \mathbf{r}_j)$ is called the coupling constant, $\mathbf{r} = \mathbf{r}_i - \mathbf{r}_j$, and \hat{r}_α is the α th component of the unit vector $\hat{\mathbf{r}}$.

The exact inclusion of the Hamiltonian in the calculation of the TPAS is a very challenging subject. Therefore, we use the mean-field theory^{33,34} where the electric field E_M created by all the other dipoles on the i th dipole is expressed as³³

$$E_\alpha^M = - \left\langle \frac{1}{2} \sum_j \sum_\beta J_{\alpha\beta}(\mathbf{r}_i - \mathbf{r}_j) \mu_\beta(\mathbf{r}_j) \right\rangle, \quad (3)$$

$$E_\alpha^M = \frac{\lambda P_\alpha}{3\epsilon_0}, \quad (4)$$

where $\langle \cdots \rangle$ is the quantum statistical ensemble average. The mean field E_M in Eq. (4) has been evaluated in textbooks^{33,34} by using the method of Lorentz. Here, P_α is the α th component of the polarization vector \mathbf{P} and λ is a constant which is taken as unity.^{24,27,33,35}

Following the method of Ref. 35, the DDI Hamiltonian can be expressed in terms of the raising σ_{32}^+ and the lowering σ_{32}^- operators for the selected induced dipole transition $|2\rangle \leftrightarrow |3\rangle$. After some mathematical manipulation, we get the DDIST Hamiltonian as

$$H_d = -(\Lambda_{32} \sigma_{32}^+ + \Lambda_{32}^* \sigma_{32}^-), \quad (5)$$

where $\sigma_{32}^+ = |3\rangle\langle 2|$ and $\sigma_{32}^- = |2\rangle\langle 3|$. The variable Λ_{32} is obtained as

$$\Lambda_{32} = \frac{2N_0 \lambda \mu_{32}^2}{3\epsilon_0} \rho_{32}, \quad (6)$$

where N_0 is of the number particles per unit volume and ϵ_0 is the dielectric constant of the medium. ρ_{32} and μ_{32} are the elements of the density matrix ρ and the dipole moment μ corresponding to the transition $|2\rangle \leftrightarrow |3\rangle$.

The nanoparticles are also interacting with the polaritonic material. Levels $|2\rangle$ and $|3\rangle$ decay to levels $|1\rangle$ and $|2\rangle$, respectively. The polaritonic material has an energy gap between energies ϵ_v and ϵ_c , where the former is the uppermost energy of the lower band and the latter is the lowest energy of the upper band. Following Ref. 14, the interaction Hamiltonian is written as

$$H_{int} = \int_C \frac{d\epsilon_k}{2\pi} [\sqrt{\gamma_2} Z_2(\epsilon_k) p(\epsilon_k) \sigma_{21}^+ + \sqrt{\gamma_3} Z_3(\epsilon_k) p(\epsilon_k) \sigma_{32}^+] + \text{H.c.}, \quad (7)$$

$$Z_i(\epsilon_k) = \frac{(\epsilon_v - \epsilon_k)^2}{(\epsilon_c - \epsilon_k)^2 + \kappa^2}, \quad (8)$$

where H.c. stands for the Hermitian conjugate and κ is a constant. The operators $p(\epsilon_k)$ and $p^\dagger(\epsilon_k)$ denote the annihilation and creation of polaritons with energy ϵ_k , respectively. γ_2 and γ_3 are constants.¹⁴ The integration contour C consists of two intervals: $-\infty < \epsilon \leq \epsilon_v$ and $\epsilon_c \leq \epsilon < \infty$. The function $Z_i(\epsilon_k)$ is known as the form factor and is obtained in Ref. 14 for a polaritonic material. In the rest of the paper, all energies are measured with respect to an energy parameter γ_0 , which can be taken as the linewidth of an atomic level in free space.

The three levels $|1\rangle$, $|2\rangle$, and $|3\rangle$ of a nanoparticle are taken in cascade configuration²⁹ where two-photon absorption takes place. Levels $|2\rangle$ and $|1\rangle$ are driven by a probe-laser field of energy ϵ_p and Rabi energy x_p . A control-laser field of energy ϵ_c and Rabi energy x_c is applied between the two excited levels $|3\rangle$ and $|2\rangle$. Using Eqs. (5) and (7) and the density-matrix method of Ref. 29, the following equations of motion for the density-matrix elements are obtained:

$$\frac{d\rho_{11}}{d\tau} = Z_2^2 \rho_{22} + ix_s(\rho_{21} - \rho_{12}), \quad (9a)$$

$$\begin{aligned} \frac{d\rho_{22}}{d\tau} = & -Z_2^2 \rho_{22} - ix_s(\rho_{21} - \rho_{12}) + ix_p(\rho_{32} - \rho_{23}) \\ & + i(\Lambda_{32}^* \rho_{32} - \Lambda_{32} \rho_{23}), \end{aligned} \quad (9b)$$

$$\frac{d\rho_{33}}{d\tau} = -Z_3^2 \rho_{33} - ix_p(\rho_{32} - \rho_{23}) - i(\Lambda_{32}^* \rho_{32} - \Lambda_{32} \rho_{23}), \quad (9c)$$

$$\frac{d\rho_{21}}{d\tau} = (i\delta_{21} - Z_{21}^2) \rho_{21} - ix_s(\rho_{22} - \rho_{11}) + ix_p \rho_{31} + i\Lambda_{32} \rho_{31}, \quad (9d)$$

$$\frac{d\rho_{31}}{d\tau} = (i\delta_{31} - Z_{31}^2)\rho_{31} - ix_s\rho_{32} + ix_p\rho_{21} + i\Lambda_{32}\rho_{21}, \quad (9e)$$

$$\begin{aligned} \frac{d\rho_{32}}{d\tau} &= (i\delta_{32} - Z_{32}^2)\rho_{32} - ix_s\rho_{31} - ix_p(\rho_{33} - \rho_{22}) \\ &\quad - i\Lambda_{32}(\rho_{33} - \rho_{22}), \end{aligned} \quad (9f)$$

where $\tau = \gamma_0 t / \hbar$, $\delta_{21} = (\varepsilon_p - \varepsilon_{21}) / \gamma_0$, $\delta_{32} = (\varepsilon_c - \varepsilon_{32}) / \gamma_0$, and $\delta_{31} = \delta_{21} + \delta_{32}$. The ε_{ij} is the resonance energy for transition $|i\rangle \leftrightarrow |j\rangle$, where i and j stand for the three levels. The functions Z_{ij}^2 are defined as

$$\begin{aligned} Z_{32}^2 &= \frac{1}{2}[Z_3^2(\varepsilon_{32}) + Z_2^2(\varepsilon_{21})], \\ Z_{31}^2 &= \frac{1}{2}Z_3^2(\varepsilon_{32}), \quad Z_{21}^2 = \frac{1}{2}Z_2^2(\varepsilon_{21}), \end{aligned} \quad (10)$$

where the square of the form factor (SFF) Z_i^2 is obtained from Eq. (8).

Two-photon absorption occurs when electrons are transferred from level $|1\rangle$ to level $|3\rangle$ via level $|2\rangle$. The density-matrix element ρ_{33} gives a measure of the population in level $|3\rangle$ due to two-photon absorption. The TPAS is calculated from ρ_{33} . We denote the absorption spectrum by I in the rest of the paper.

From Eq. (9c), we obtained the following expression for TPAS in the steady state:

$$I = \frac{2x_c}{\gamma_3} \text{Im}(\rho_{32}). \quad (11)$$

Note that the last term in Eq. (9c) gives zero contribution when Λ_{32} from Eq. (6) is substituted. The above equation can be calculated numerically by solving Eqs. (9a)–(9f) using a Runge-Kutta method in MAPLE. However, we want to get an analytical expression for TPAS in the steady state.

Let us first obtain an expression for the TPAS in the absence of DDIST. We have considered that the control field x_c is weaker than the probe field x_p . Therefore, we have evaluated the density-matrix element ρ_{32} in the first order of control field x_c . However, all the orders of x_p are included in the formulation. This means that nonlinear effects due to the probe field are included in the calculation.

After rigorous mathematical manipulations, we have derived the following expression for ρ_{32} from Eqs. (9a)–(9f):

$$\rho_{32} = ix_c X, \quad (12)$$

where the function X is obtained as

$$X = \frac{2Z_{21}^2(2x_p^4 - d_{31}d_{21}x_p^2) - (4Z_{21}^2x_p^4 + Z_2^2x_p^2|d_{21}|^2)}{d_{21}(d_{32}d_{31} + ix_p^2)(4Z_{21}^2x_p^2 + Z_2^2|d_{21}|^2)} \quad (13)$$

and

$$d_{21} = i\delta_{21} - Z_{21}^2, \quad d_{31} = i\delta_{31} - Z_{31}^2, \quad d_{32} = i\delta_{32} - Z_{32}^2. \quad (14)$$

Putting Eq. (12) into Eq. (11), the following expression for the TPAS is obtained after further mathematical manipulations:

$$I = I_0 \left[\frac{A(Z_{31}^2\delta_{32} + \delta_{31}Z_{32}^2) + B(Z_{31}^2Z_{32}^2 - \delta_{31}\delta_{32} + x_p^2)}{(Z_{31}^2Z_{32}^2 - \delta_{31}\delta_{32} + x_p^2)^2 + (Z_{31}^2\delta_{32} + \delta_{31}Z_{32}^2)^2} \right], \quad (15)$$

where $I_0 = 2x_c^2 / Z_3^2$ and the functions A and B are obtained as

$$\begin{aligned} A &= \frac{Z_3^2(2\delta_{31}Z_{21}^2x_p^2 - \delta_{21}Z_2^2x_p^2)}{4Z_{21}^2x_p^2 + Z_2^2(\delta_{21}^2 + Z_{21}^4)}, \\ B &= \frac{Z_3^2(2Z_{21}^2Z_{31}^2x_p^2 + Z_2^2Z_{21}^2x_p^2)}{4Z_{21}^2x_p^2 + Z_2^2(\delta_{21}^2 + Z_{21}^4)}. \end{aligned} \quad (16)$$

The physics behind Eq. (15) is that it gives the TPAS when electrons are transferred from level $|1\rangle$ to level $|3\rangle$ via level $|2\rangle$. When the probe-laser field of energy ε_p and the control-laser field of energy ε_c are in resonance with the transitions $|2\rangle \leftrightarrow |1\rangle$ and $|3\rangle \leftrightarrow |2\rangle$, respectively, Eq. (15) has a peak at the detuning parameter $\delta_{31} = 0$. The width and the height of the peak depend on the SFF functions Z_2^2 and Z_3^2 .

Similarly, in the presence of the DDIST, we have also obtained the expression for ρ_{32} from Eqs. (9a)–(9c) in the steady state:

$$\rho_{32} = ix_c \frac{X}{1 - C_\lambda X}, \quad (17)$$

where the DDI parameter C_λ is

$$C_\lambda = \frac{2N_0\lambda\mu_{32}^2}{3\epsilon_0\gamma_0}. \quad (18)$$

This parameter measures the strength of the DDIST and has been widely used in the literature.^{24,27,35}

Finally, the expression for the TPAS in the presence of the DDIST can be obtained by putting Eq. (17) into Eq. (11):

$$I = I_0 \left(\frac{\Pi_a \Pi_d}{(\Pi_d - C_\lambda \Pi_b)^2 + (C_\lambda \Pi_a)^2} \right), \quad (19)$$

where functions Π_a , Π_b , and Π_c are obtained as

$$\begin{aligned} \Pi_a &= A(Z_{31}^2\delta_{32} + \delta_{31}Z_{32}^2) + B(Z_{31}^2Z_{32}^2 - \delta_{31}\delta_{32} + x_p^2), \\ \Pi_b &= A(Z_{31}^2Z_{32}^2 - \delta_{31}\delta_{32} + x_p^2) - B(Z_{31}^2\delta_{32} + \delta_{31}Z_{32}^2), \\ \Pi_d &= (Z_{31}^2Z_{32}^2 - \delta_{31}\delta_{32} + x_p^2)^2 + (Z_{31}^2\delta_{32} + \delta_{31}Z_{32}^2)^2. \end{aligned} \quad (20)$$

Note that when we put $C_\lambda = 0$, we get back the expression of the two-photon absorption in the absence of DDIST [see Eq. (15)].

The physics behind Eq. (21) is that it gives the TPAS in the presence of the DDI when electrons are transferred from level $|1\rangle$ to level $|3\rangle$ via level $|2\rangle$. It is important to note that Eq. (19) does not have a peak at the detuning parameter

$\delta_{31}=0$ when the probe- and control-laser fields are resonant with the transitions $|2\rangle \leftrightarrow |1\rangle$ and $|3\rangle \leftrightarrow |2\rangle$, respectively. On the other hand, Eq. (15) gives a peak at $\delta_{31}=0$. This means that there is an inhibition of two-photon absorption in the system due to the DDIST. Equation (21) gives two peaks which are located at the right- and left-hand sides of $\delta_{31}=0$. This phenomenon can be explained by using the idea of dressed states which are discussed below. One can also see from Eq. (21) that the heights of both peaks decrease as the DDI parameter C_λ increases. In other words, the intensity of the two-photon absorption process decreases when the nanoparticles are interacting with each other via DDIST.

Note that when $C_\lambda = \Pi_d / \Pi_b$, Eq. (19) reduces to

$$I = I_0 \left(\frac{\Pi_d}{C_\lambda^2 \Pi_a} \right). \quad (21)$$

The above expression tells us that the height and the width of the absorption peaks of the spectrum depend on the quantities C_λ , Π_a , and Π_d .

In the next section, we have performed numerical simulations when the DDIST is stronger than the probe and coupling fields. In this situation, dressed states are created in the system due to the strong coupling between levels $|2\rangle$ and $|3\rangle$. The analysis of the dressed states is needed to understand the phenomenon of two-photon absorption in the next section.

We consider the following Hamiltonian:

$$H = (\delta_{21}\sigma_{22} + \delta_{31}\sigma_{33}) - (x_c\sigma_{32}^+ + x_p\sigma_{21}^+) - C_\lambda\rho_{32}\sigma_{32}^+ + \text{H.c.}, \quad (22)$$

where $\sigma_{22} = |2\rangle\langle 2|$ and $\sigma_{33} = |3\rangle\langle 3|$. Note that the above Hamiltonian is written in unitless quantities. The first, second, and third terms correspond to a nanoparticle, particle-laser field interaction, and the DDIST, respectively. Wave functions of the above Hamiltonian can be written as a linear combination of three states, $|1\rangle$, $|2\rangle$, and $|3\rangle$, which form a basis set.

After some mathematical manipulation, we found the following eigenvalues:

$$\varepsilon_\pm = (\delta_{21} + \delta_{32}/2) \pm \sqrt{(\delta_{32}/2)^2 + 4C_\lambda^2|\rho_{32}|^2}. \quad (23)$$

Note that we have neglected the effect of the probe and coupling fields in the evaluation of the above equations. The corresponding wave functions are obtained as

$$|\pm\rangle = \frac{C_\lambda|\rho_{32}|}{\sqrt{(\varepsilon_\pm - \delta_{31})^2 + C_\lambda^2|\rho_{32}|^2}}|2\rangle + \frac{(\varepsilon_\pm - \delta_{31})}{\sqrt{(\varepsilon_\pm - \delta_{31})^2 + C_\lambda^2|\rho_{32}|^2}}|3\rangle. \quad (24)$$

The wave functions $|+\rangle$ and $|-\rangle$ are called the dressed states or symmetric and antisymmetric states, respectively. The dressed states due to the DDI have also been calculated in the literature.¹⁹

III. NUMERICAL SIMULATIONS

In this section, numerical simulations are performed on a SiC crystal which is a polaritonic band-gap material.¹³ The energy-band parameters ε_v and ε_c are taken as $\varepsilon_v = 98$ meV

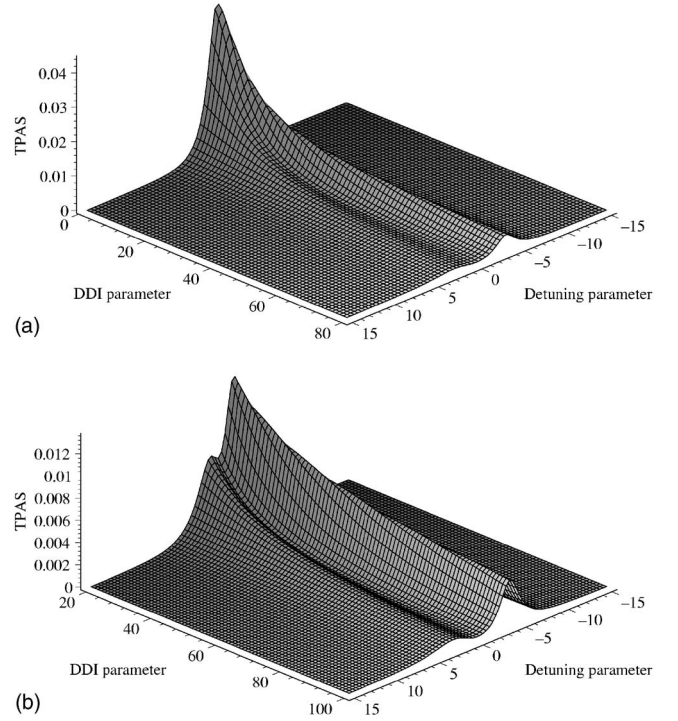


FIG. 2. The plot of normalized two-photon absorption spectrum (I/I_0) as function of the detuning parameter δ_{31} and the DDI parameter C_λ . The probe field is taken as $x_c=1$ and the resonance energy is taken as $\varepsilon_{32}=0.5\varepsilon_v$. Note that the single peak at zero detuning splits into two peaks in the presence of the DDIST.

and $\varepsilon_c = 118$ meV.¹³ Polaritonic crystals are generally characterized by their gap to midgap ratios. The gap to midgap ratio for SiC is about 18.3%.

We consider that the resonance energy for the decay transitions $|2\rangle \leftrightarrow |1\rangle$ lies in the upper band (i.e., $\varepsilon_{21} = 1.5\varepsilon_v$). The findings of this work are not affected whether the resonance energy ε_{21} lies in the lower band or in the upper band. However, the resonance energy ε_{32} for the decay transition $|3\rangle \leftrightarrow |2\rangle$ will be varied within the lower band. The parameters γ_2 and γ_3 appearing in the form factors are taken as $0.1\gamma_0$. We have considered that the coupling field is tuned with the transition $|3\rangle \leftrightarrow |2\rangle$ (i.e., $\delta_{32}=0$).

The three-dimensional figure for the normalized two-photon absorption (I/I_0) has been plotted in Figs. 2(a) and 2(b) as function of the detuning parameter δ_{21} and the DDI parameter C_λ . The decay resonance energy ε_{32} is taken at the middle of the lower band. The Rabi energy for the probe field is taken as $x_p=1$. Note that in Fig. 2(a) the spectrum has a peak at zero detuning in the absence of DDIST. This peak corresponds to two-photon absorption in the nanoparticles.

It is interesting to note that as the DDI parameter increases, the peak located at the zero detuning point splits into two. These two peaks are located on the right- and left-hand sides of the zero detuning point in the presence of the DDIST. We have plotted Fig. 2(b) for larger values of the DDI parameter. As a result, the peaks are more pronounced than those in Fig. 2(a). The right-hand peak is stronger than the left-hand peak. The heights of the peaks decrease as the DDI parameter increases. This is because the heights are

inversely proportional to the DDI parameter [see Eq. (21)].

Note that at large values of the DDI parameter, the minimum between the two peaks has almost a zero value. This minimum corresponds to the inhibition of two-photon absorption due to the DDIST. This is an interesting finding of the present work.

It is interesting to note that two-photon absorption has also been studied in multilevel atomic gases. By varying the strengths and phases of the laser fields, the inhibition of two-photon absorption has been predicted.^{36,37} However, the effect of DDI has not been investigated in these references.

The mechanism behind two-photon inhibition due to DDIST can be explained by using a theory of dressed states which was discussed in the preceding section. In the absence of DDIST, there are no dressed states in the system and only one route ($|1\rangle \rightarrow |2\rangle \rightarrow |3\rangle$) is available for the absorption of two photons. In other words, the route $|1\rangle \rightarrow |2\rangle$ is available for a probe field photon, whereas the route $|2\rangle \rightarrow |3\rangle$ is available for a control field photon.

It is worth emphasizing that the probe field monitors the two-photon absorption spectrum through the transition $|1\rangle \rightarrow |2\rangle$ by varying the detuning parameter δ_{21} . That is why in the absence of the DDIST, we get one absorption peak due to the transition $|1\rangle \rightarrow |2\rangle$ at zero detuning (i.e., $\delta_{21}=0$).

However, in the presence of the DDIST, the system has two dressed states ($|+\rangle$ and $|-\rangle$). Now, the probe field photon has two routes, $|1\rangle \rightarrow |+\rangle$ and $|1\rangle \rightarrow |-\rangle$. Therefore, there are two routes ($|1\rangle \rightarrow |-\rangle \rightarrow |3\rangle$ and $|1\rangle \rightarrow |+\rangle \rightarrow |3\rangle$) which are available for the two-photon absorption process. When the detuning parameter lies on the right-hand side of the zero detuning point (i.e., $\delta_{21} > 0$), the two-photon absorption occurs due to the route $|1\rangle \rightarrow |+\rangle$ (or $|1\rangle \rightarrow |+\rangle \rightarrow |3\rangle$). This is why we get the right-hand peak in the spectrum. Similarly, when δ_{21} lies to the left-hand side of the zero detuning point (i.e., $\delta_{21} < 0$), the absorption occurs due to the route $|1\rangle \rightarrow |-\rangle$ (or $|1\rangle \rightarrow |-\rangle \rightarrow |3\rangle$) and the left-hand peak appears in the spectrum.

At zero detuning (i.e., $\delta_{21}=0$), the energy difference between the two routes $|1\rangle \rightarrow |-\rangle \rightarrow |3\rangle$ and $|1\rangle \rightarrow |+\rangle \rightarrow |3\rangle$ is zero. Therefore, these routes interfere with each other and the inhibition of two-photon absorption occurs. This is why we get a minimum which corresponds to the inhibition of two-photon absorption in the system.

Note that the energy splitting ($\epsilon_+ - \epsilon_-$) of the dressed states depends not only on the DDI parameter C_λ but also on ρ_{32} . Furthermore, ρ_{32} depends on the functions Z_2^2 and Z_3^2 and the probe Rabi energy x_p [see Eq. (12)]. This is why we found that the height of the minimum and the separation between the two peaks depend on C_λ and x_p .

The theory of dressed states has also been used to explain the effect of the DDI in quantum optics,^{30,31} photonic crystals,³² and quantum dots. For example, Lukin and Hemmer³⁰ have used the dressed state theory for the DDIST to explain quantum entanglement in two three-level and four-level atoms. In a previous work, we have also used the idea of dressed states due to DDIST in four-level atoms doped in photonic crystals.³² Petrosyan and Kurizki⁹ have considered the splitting of energy states into symmetric and asymmetric states (dressed states) due to the DDI in quantum dots. The theory of dressed states has also been applied by Gea-

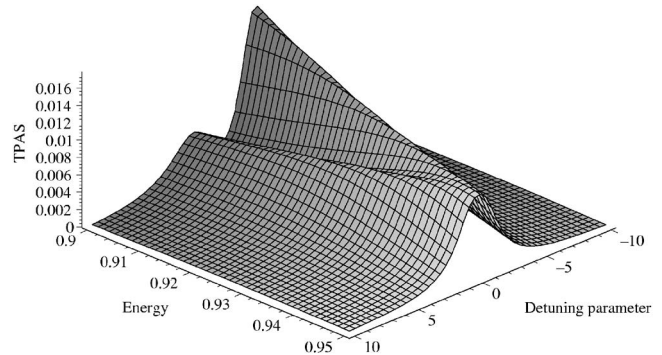


FIG. 3. The plot of normalized two-photon absorption spectrum (I/I_0) as function of the detuning parameter δ_{31} and the energy. For the control field, and the resonance energy and the DDI parameter are taken as $x_p=1$ and $C_\lambda=50$, respectively. Note that the two peaks merge into one near the band edge.

Banacloche *et al.*¹⁷ in arrays of quantum dots. They showed that the quantum dots have three-level and four-level structures due to dressed states created by the DDI.

The role of the decay transition $|3\rangle \rightarrow |2\rangle$ has also been investigated on the TPAS. The results are shown in Fig. 3 as functions of the resonance energy and DDI parameter. Interesting results are found when the resonance energy gets near the band edge. Note that the right and left absorption peaks merge into a single peak which is located at zero detuning. This means that the inhibition of two-photon absorption disappears when the resonance energy lies near the band edge. In other words, the phenomenon of two-photon absorption can be switched on and off by tuning the resonance energy within the lower band of the crystal.

The basic idea behind the above phenomenon can be explained as follows. Note that the linewidth of level $|3\rangle$ is due to the decay transition $|3\rangle \rightarrow |2\rangle$ and is calculated from the SFF $Z_3^2(\epsilon_{32})$. The SFF has been plotted as a function of the resonance energy in Fig. 4. Note also that the SFF has a large value near the edge of the lower band and a small value near the upper band edge. The width and the height of the absorption peaks depend on the linewidths of level $|3\rangle$. When the resonance energy ϵ_{32} lies near the band edge, $Z_3^2(\epsilon_{32})$ has a very large value (see Fig. 4). The broadening of level $|3\rangle$ is larger than the energy splitting due to the DDIST. Therefore,

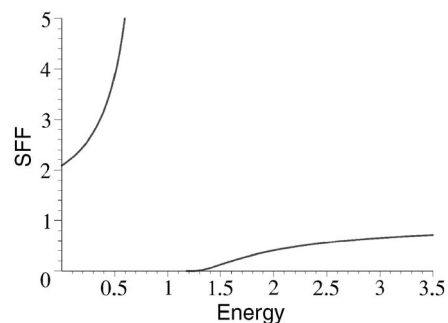


FIG. 4. The plot of the function SFF as a function of energy ϵ/ϵ_v . The energy-band parameters are taken as $\epsilon_v=98$ meV, $\epsilon_c=118$ meV, and $\kappa=10^{-3}\epsilon_v$. The energy gap lies between ϵ_v and ϵ_c . Note that the SFF has a large value near the lower band edge.

the two peaks merge into one and the inhibition of the two-photon absorption disappears at zero detuning.

Note that the switching phenomenon cannot be observed if the resonance energy lies in the upper band since the function $Z_3^2(\epsilon_{32})$ has a very small value at the upper band edge (see Fig. 4).

The reader may recall that the above calculations are performed when the coupling field is tuned with the transition $|3\rangle \rightarrow |2\rangle$. In other words, we have put $\delta_{32}=0$ in $\delta_{31}=\delta_{21}+\delta_{32}$. However, if we consider that the probe field is tuned with the transition $|2\rangle \rightarrow |1\rangle$ (i.e., $\delta_{21}=0$), we will not be able to see the inhibition effect. It is because there is no DDIST effect due to the transition $|2\rangle \rightarrow |1\rangle$ and the dressed level splitting cannot be probed by the coupling field.

Recently, Scalora and Bowden³⁸ have shown that when the propagation effects in the study of ultrafast switching are not important in a dense medium, the mean-field theory (MFT) method is valid when dealing with DDI. They showed that when the propagation effects are important, density-matrix equations such as Eq. (9) should be supplemented by Maxwell's equations. These equations must be solved self-consistently to calculate the local electric field and nanoparticle variables. In the present work, the propagation effects are not important, and therefore, the MFT is valid.

We would like to discuss the limitations of the MFT method used in the present work. One of the main limitations is that the theory ignores the fluctuations due to the DDI produced in the system.^{33,34} The individual dipole of a nanoparticle is interacting only with the mean field of all the other dipoles in the photonic crystal [see Eq. (3)]. In some physical phenomena, such as phase transition, the fluctuations become important near the critical point. However, the MFT method usually gives correct qualitative predictions for the phase transition in three-dimensional systems. In the present work, as we are not studying phase transition or similar phenomena, the MFT method is valid and provides qualitative results. To get quantitative results for the present problem, one has to go beyond the MFT method such as the random-phase approximation.

It is worth mentioning that the shortcomings of the MFT method are often mentioned at great lengths in the literature. However, one should also emphasize the successes and the wide range of applicability of the theory.^{33,34} For example, the MFT method has been extensively used in studying interacting systems such as gases, liquids, solids, fermions, and bosons. The theory provides a feasible and useful approach for complicated problems such as the calculation of the DDI in the present paper. In fact, it is quite often the only theory available for understanding the physics of interacting systems. It is found that many numerical approaches become more difficult as the dimensionality increases, which is not the case for the MFT method.

The findings of the present theory are valid not only for SiC but also for all different types of polaritonic crystals such as SiC, GaP, GaAs, CdTe, CdSe, InAs, MgO, NaF, etc. This is due to the fact that the results presented in the paper depend on the form factor, which in turn depends on the band gap of the crystal. Since all polaritonic crystals have band gaps, the findings in the paper are valid irrespective of the choice of polaritonic crystal.

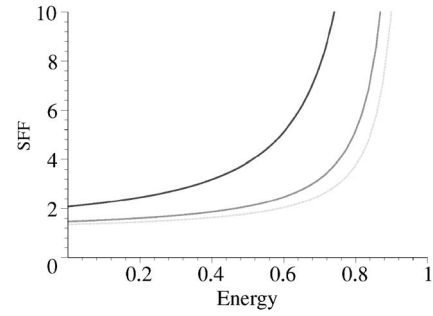


FIG. 5. The plot of the function SFF as a function of energy (ϵ/ϵ_v) for SiC, GaP, and GaAs when the resonance energy lies within the lower band. The values of ϵ_v and ϵ_c are taken, respectively, as 98 and 118 meV for SiC, 45.5 and 50.1 meV for GaP, and 33.6 and 36.2 meV for GaAs. The solid, dash, and dash-dotted lines correspond to SiC, GaP, and GaAs, respectively.

Note that the expressions for the TPAS given in Eqs. (19) and (21) depend on the SFF functions Z_3^2 and Z_2^2 , where Z is called the form factor and is given in Eq. (8). The form factor depends on the values of ϵ_v and ϵ_c or the gap to midgap ratio R_{gm} , which is defined as

$$R_{gm} = \frac{\epsilon_c - \epsilon_v}{(\epsilon_c + \epsilon_v)/2}.$$

In short, the function SFF depends on the physical parameters of the polaritonic material. The values of ϵ_v and ϵ_c are taken, respectively, as 45.5 and 50.1 meV for GaP and 33.6 and 36.2 meV for GaAs.¹³ Using the above equation, it is found that the gap to midgap ratios for SiC, GaP, and GaAs are 18%, 9.7%, and 7.5%, respectively.

We have plotted the function SFF for SiC, GaP, and GaAs in Fig. 5 when the resonance energies lie within the lower band of the respective crystals. The solid, dashed, and dash-dotted lines correspond to SiC, GaP, and GaAs, respectively. One can see from Fig. 5 that for a given value of the resonance energy, the SFF has the largest value for SiC and the lowest value for GaP. Note that the gap to midgap ratio for SiC is larger than that of GaAs. Therefore, one can say that the SFF has larger value for materials which have larger gap to midgap ratio and vice versa.

We have performed numerical simulations on TPAS for the three materials. The results are presented here. It is found that the qualitative features of TPAS remain the same for all three materials. However, it is seen that the heights of the peaks have their largest values for SiC and the smallest for GaP. Similarly, the resonance energy at which the two peaks merge into one (i.e., the critical resonance energy) has its largest value for SiC and the smallest for GaAs. It means that the heights of the peaks are inversely proportional to the gap to midgap ratio, whereas the critical resonance energy is directly proportional to it.

ACKNOWLEDGMENTS

The author is thankful to NSERC of Canada for financial support in the form of a research grant. The author is also thankful to I. Haque for proofreading the paper.

- ¹A. M. Steane, Rep. Prog. Phys. **61**, 117 (1998); M. A. Nielsen and I. L. Chuang, *Quantum Computation and Quantum Information* (Cambridge University Press, Cambridge, 2000).
- ²D. Harrison, *Quantum Wells, Wires and Dots* (Wiley, New York, 2001); D. Bimberg, M. Grundmann, and N. N. Ledentsov, *Quantum Dot Heterostructures* (Wiley, Chichester, 1999).
- ³M. Bayer, O. Stern, P. Hawrylak, S. Fafard, and A. Forchel, Nature (London) **405**, 923 (2000); H. Kamada, H. Gotoh, J. Temmyo, T. Takagahara, and H. Ando, Phys. Rev. Lett. **87**, 246401 (2001); P. Michler, A. Imamoglu, M. D. Mason, P. J. Carson, G. F. Strouse, and S. K. Buratto, Nature (London) **406**, 968 (2000); D. V. Regelman, U. Mizrahi, D. Gershoni, E. Ehrenfreund, W. V. Schoenfeld, and P. M. Petroff, Phys. Rev. Lett. **87**, 257401 (2001); P. Michler, A. Kiraz, C. Becher, W. V. Schoenfeld, P. M. Petroff, L. Zhang, E. Hu, and A. Imamoglu, Science **290**, 2282 (2000); W. W. Chow, H. C. Schneider, and M. C. Phillips, Phys. Rev. A **68**, 053802 (2003); J. F. Dynes, M. D. Frogley, M. Beck, J. Faist, and C. C. Phillips, Phys. Rev. Lett. **94**, 157403 (2005).
- ⁴A. Barenco, D. Deutsch, A. Ekert, and R. Jozsa, Phys. Rev. Lett. **74**, 4083 (1995).
- ⁵S. F. Wuister, C. de Mello Donega, and A. Meijerink, J. Chem. Phys. **121**, 4310 (2004), and references therein.
- ⁶X. Wang and C. Shih, Appl. Phys. Lett. **88**, 113114 (2006), and references therein.
- ⁷Ling Xu, Jun Xu, Zhongyuan Ma, Wei Li, Xinfan Huang, and Kunji Chen, Appl. Phys. Lett. **89**, 033121 (2006), and references therein.
- ⁸H. T. Dung, L. Knoll, and D. G. Welsch, Phys. Rev. A **66**, 063810 (2002), and references therein.
- ⁹D. Petrosyan and G. Kurizki, Phys. Rev. Lett. **89**, 207902 (2002), and references therein.
- ¹⁰W. Shi, Y. Zheng, H. Peng, N. Wang, C. S. Lee, and S. T. Lee, Appl. Phys. Lett. **75**, 1547 (1999).
- ¹¹N. Q. Huong and J. L. Birman, Phys. Rev. B **61**, 13131 (2000), and references therein.
- ¹²W. H. Chang, W. Y. Chen, H. S. Chang, T. P. Hsieh, J. I. Chyi, and T. M. Hsu, Phys. Rev. Lett. **96**, 117401 (2006); M. Barth, R. Schuster, A. Gruber, and F. Cichos, *ibid.* **96**, 243902 (2006), and references therein.
- ¹³C. Kittel, *Introduction to Solid State Physics* (Wiley, New York, 1986).
- ¹⁴V. I. Rupasov and Mahi R. Singh, Phys. Rev. Lett. **77**, 338 (1996); Phys. Rev. A **54**, 3614 (1997).
- ¹⁵Mahi R. Singh and W. Lau, Phys. Lett. A **231**, 115 (1997).
- ¹⁶Mahi R. Singh, J. Mod. Opt. **52**, 1857 (2007).
- ¹⁷J. Gea-Banacloche, M. Mumba, and M. Xiao, Phys. Rev. B **74**, 165330 (2006).
- ¹⁸B. W. Lovett, J. H. Reina, A. Nazir, and G. A. Briggs, Phys. Rev. B **68**, 205319 (2003).
- ¹⁹T. Unold, K. Mueller, C. Lienau, T. Elsaesser, and A. D. Wieck, Phys. Rev. Lett. **94**, 137404 (2005).
- ²⁰G. D. Sanders, K. W. Kim, and W. C. Holton, Phys. Rev. A **60**, 4146 (1999).
- ²¹S. Empedocles and M. Bawendi, Science **278**, 2114 (1997).
- ²²E. Paspalakis, A. Kalini, and A. F. Terzis, Phys. Rev. B **73**, 073305 (2006).
- ²³G. Y. Slepyan, S. A. Maksimenko, A. Hoffmann, and D. Bimberg, Phys. Rev. A **66**, 063804 (2002); Phys. Rev. B **70**, 045320 (2004).
- ²⁴P. de Vries and A. Lagendijk, Phys. Rev. Lett. **81**, 1381 (1998); S. Scheel, L. Knoll, D. G. Welsch, and S. M. Barnett, Phys. Rev. A **60**, 1590 (1999); M. Fleischhauer and S. F. Yelin, *ibid.* **59**, 2427 (1999); A. B. Matsko, I. Novikova, M. O. Scully, and G. R. Welch, Phys. Rev. Lett. **87**, 133601 (2001); O. G. Caledron, M. A. Anton, and F. Careno, Eur. Phys. J. D **25**, 77 (2003).
- ²⁵M. E. Crenshaw, M. Scalora, and C. M. Bowden, Phys. Rev. Lett. **68**, 911 (1992).
- ²⁶F. A. Hopf, C. M. Bowden, and W. H. Louisell, Phys. Rev. A **29**, 2591 (1984); J. W. Haus, L. Wang, M. Scalora, and C. M. Bowden, *ibid.* **38**, 4043 (1988); M. P. Hehlen, H. U. Gudel, Q. Shu, J. Rai, S. Rai, and S. C. Rand, Phys. Rev. Lett. **73**, 1103 (1994); C. M. Bowden, Phys. World **7** (12), 24 (1994).
- ²⁷J. P. Dowling and C. M. Bowden, Phys. Rev. Lett. **70**, 1421 (1993); A. S. Manka, J. P. Dowling, C. M. Bowden, and C. M. Fleischhauer, Quantum Opt. **6**, 371 (1994).
- ²⁸R. Friedberg, S. R. Hartmann, and J. T. Manassah, Phys. Rep., Phys. Lett. **7**, 101 (1973); **39**, 3444 (1989); **40**, 2446 (1989); J. J. Maki, M. S. Malcuit, J. E. Sipe, and R. W. Boyd, Phys. Rev. Lett. **67**, 972 (1991).
- ²⁹M. O. Scully and M. S. Zubairy, *Quantum Optics* (Cambridge University Press, Cambridge, 1997).
- ³⁰M. D. Lukin and P. R. Hemmer, Phys. Rev. Lett. **84**, 2818 (2000).
- ³¹C. Skornia, J. von Zanthier, G. S. Agarwal, E. Werner, and H. Walther, Phys. Rev. A **64**, 053803 (2001).
- ³²Mahi R. Singh, Opt. Lett. (to be published).
- ³³G. F. Mazenko, *Quantum Statistical Mechanics* (Wiley, New York, 2000).
- ³⁴H. E. Stanley, *Phase Transitions and Critical Phenomena* (Oxford University Press, New York, 1971); M. Yeomans, *Statistical Mechanics of Phase Transitions* (Clarendon Press, Oxford, 1992), Chap. 4.
- ³⁵Mahi R. Singh, private communication (2007).
- ³⁶N. Imoto, H. A. Haus, and Y. Yamamoto, Phys. Rev. A **32**, 2287 (1985); S. E. Harris and Y. Yamamoto, Phys. Rev. Lett. **81**, 3611 (1998); J. H. Zou, X. M. Hu, G. L. Cheng, X. Li, and D. Du, Phys. Rev. A **72**, 055802 (2005); W. Jiang, Q. F. Chen, Y. S. Zhang, and G. C. Guo, *ibid.* **73**, 053804 (2006).
- ³⁷G. S. Agarwal and W. Harshawardhan, Phys. Rev. Lett. **77**, 1039 (1996); J. Y. Gao, S. H. Yang, D. Wang, X. Z. Guo, K. X. Chen, Y. Jiang, and B. Zhao, Phys. Rev. A **61**, 023401 (2000); D. McGloin, J. Phys. B **36**, 2861 (2003); M. Yan, E. G. Rickey, and Y. Zhu, Phys. Rev. A **64**, 041801(R) (2001); D. A. Braje, V. Balic, G. Y. Yin, and S. E. Harris, *ibid.* **68**, 041801(R) (2003); Y. F. Chen, Z. H. Tsai, Y. C. Liu, and I. A. Yu, Opt. Lett. **30**, 3207 (2005).
- ³⁸M. Scalora and C. M. Bowden, Phys. Rev. A **51**, 4048 (1995).